Powder Technology 276 (2015) 200–203

Contents lists available at ScienceDirect

Powder Technology

journal homepage: www.elsevier.com/locate/powtec

Low frequency ultrasound assisted synthesis of $La_{0.6}Sr_{0.4}Co_{0.2}Fe_{0.8}O_{3-\delta}$ (LSCF) perovskite nanostructures

A. Akbari-Fakhrabadi [a,*], P. Sathishkumar [b,c], K. Ramam [b], R. Palma [a], R.V. Mangalaraja [b]

[a] Department of Mechanical Engineering, University of Chile, Beauchef 850, Santiago, Chile
[b] Advanced Ceramics and Nanotechnology Laboratory, Department of Materials Engineering, Faculty of Engineering, University of Concepcion, Concepcion, Chile
[c] Department of Chemistry, Periyar Maniammai University, Vallam, Thanjavur, Tamil Nadu, India

ARTICLE INFO

Article history:
Received 5 November 2014
Received in revised form 10 January 2015
Accepted 22 February 2015
Available online 28 February 2015

Keywords:
42 kHz ultrasound
LSCF
Nanostructures
Powder characteristics

ABSTRACT

$La_{0.6}Sr_{0.4}Co_{0.2}Fe_{0.8}O_{3-\delta}$ (LSCF) perovskite nanostructures were synthesised using a 42 kHz ultrasound assisted synthesis technique for the fabrication of electrodes in the intermediate and/or low temperature solid oxide fuel and electrolysis cells (SOFCs/SOECs). The obtained nanomaterials were dried at 110 °C followed by calcination in a normal atmosphere at various temperatures from 400 to 1000 °C for 2 h. Powder characteristics such as crystal structure, thermal decomposition, particle size and morphology were analysed. The transmission electron microscopy (TEM) study revealed the uniform equi-axial shape and growth of the obtained nanostructures with respect to the calcination temperature till 800 °C. The structural and chemical analyses confirmed the existence of LSCF and $CoFe_2O_4$ phases.

1. Introduction

$La_{1-x}Sr_xCo_yFe_{1-y}O_{3-\delta}$ ($0 \le x \le 0.5$ and $0 \le y \le 0.8$, LSCFs) are well-known mixed ionic and electronic conductive (MIEC) materials which are attractive for solid oxide fuel cells (SOFCs) and solid oxide electrolyser cells (SOECs) as electrodes and oxygen separation membranes [1–4]. The perovskite-structured LSCF electrode materials with large La and Sr cations occupying the A-sites are more interesting candidates for the SOFC and SOEC. The smaller Co and Fe cations are reported to preferably populate the B-site in the ABO_3 structure [5]. The chemical composition, temperature and defect concentration of the perovskites may lead to crystallize the orthorhombic, rhombohedral as well as cubic structures [6,7]. Properties such as gas permeability, ionic and electronic conductivities depend on their structure and composition, which are influenced by the synthetic procedure [8]. The perovskite-structured LSCF nanomaterials have been prepared by various synthesis routes like conventional solid state reaction [8,9], combustion synthesis [9–13], sol–gel [14,15], precipitation [16], reverse micelle technique [17], Pechini method [18] citrate–hydrothermal synthesis [19] and hydrothermal synthesis [16]. In addition to that, the perovskite oxides such as $LaMnO_3$ [20], $La_{0.7}Sr_{0.3}MnO_3$ [21] and $GdCo_{1-x}Cu_xO_{3-\delta}$ [22] have been synthesised by a sonochemical method, which has recently been used to prepare the various nanocrystalline materials including metals and ceramics [23].

On the other hand, sonochemistry is a research area which uses the power of ultrasound to enhance synthetic and catalytic processes for the preparation of novel nanomaterials by increasing reaction rates. When an ultrasonic wave passes through the liquid medium, microbubbles are generated which tend to implode and collapse violently in the liquid, leading to the formation of high velocity jets of liquid and the release of a large amount of energy [23,24].

In this work, a low frequency ultrasound (42 kHz) assisted synthesis of $La_{0.6}Sr_{0.4}Co_{0.2}Fe_{0.8}O_{3-\delta}$ nanomaterials was performed. The characteristics such as crystal structure, changes of phase and composition, particle size and morphology of the resulted nanostructures are investigated using various characterisation techniques.

2. Experimental

The stoichiometric proportions of La, Sr, Co and Fe nitrate precursors were dissolved in double distilled water under vigorous stirring in order to obtain a homogeneous solution. 20% NaOH solution was added dropwise to the precursor solution under vigorous stirring along with the ultrasonic irradiation (42 kHz; 8890, Cole-Parmer, USA). The role of NaOH was to maintain the pH during the synthesis of $La_{0.6}Sr_{0.4}Co_{0.2}Fe_{0.8}O_{3-\delta}$ nanomaterials. The ultrasonic irradiation was continued for an hour until the completion of the formation of $La_{0.6}Sr_{0.4}Co_{0.2}Fe_{0.8}O_{3-\delta}$ perovskite nanostructures. The subsequent filtration of the obtained material was performed using 0.45 μm nylon membrane. The filtered residues were re-dispersed and washed with double distilled water for several times until the washed solution reached neutral pH. Finally, the obtained materials were dried at

* Corresponding author.
E-mail address: aliakbarif@ing.uchile.cl (A. Akbari-Fakhrabadi).

http://dx.doi.org/10.1016/j.powtec.2015.02.043
0032-5910/

110 °C and then calcined in the normal atmosphere at various temperatures of 400, 600, 800 and 1000 °C for 2 h.

The thermal analysis of the as-dried materials were characterised by thermo-gravimetric (TG) and differential scanning calorimetry (DSC) analyses using Netzsch-STA 449C and Netzsch DSC 404F3, respectively.

The calcined nanopowders were characterised by X-ray diffraction (XRD, Bruker D8) and transmission electron microscopy (TEM, Tecnai F20 FEG operated at 200 kV, equipped with an EDS detector) analyses to study their structure and particle size and for chemical analysis.

3. Results and discussion

The XRD patterns of the nanopowders calcined at 400, 600, 800 and 1000 °C for 2 h are shown in Fig. 1. The diffraction peaks appearing in the LSCF samples calcined at 600, 800 and 1000 °C were indexed according to the rhombohedral symmetry with the R-3c space group. As can be seen, the additional peaks detected at 800 and 1000 °C may be indexed as $CoFe_2O_4$. The calculated lattice parameter of LSCF (a = 5.5265 and c = 13.4643 Å, obtained by Rietveld refinement using Topas 4.2. software) is lower than the theoretical lattice parameter (a = 5.4451 and c = 13.2553 Å, JCPDS # 48-0124), which can be attributed to B-site cation (Co and Fe) deficiency in the ABO_3 perovskite structure of LSCF [1]. At a lower calcination temperature of 400 °C, LSCF peaks do not exist but some peaks which can also be detected in the XRD pattern of the sample calcined at 600 °C, were indexed as $La_2O_2CO_3$.

The crystallite sizes were calculated from the X-ray broadening technique using Scherrer equation on the best-resolved diffraction peak [25]:

$$D = \frac{0.9\lambda}{\left(\beta^2_{sample} - \beta^2_{ref}\right)^{1/2}} \cos\theta$$

where, D is the crystallite size diameter (in nm), λ = 1.54 Å, β is the full width at half maximum (FWHM) of a diffraction peak, (110), and β_{ref} corresponds to the instrumental FWHM. The crystallite sizes were found to be 30.1, 32.3 and 38.3 nm for LSCF nanopowders calcined at 600, 800 and 1000 °C, respectively. The increase in the crystallite size with calcination temperature shows its crystal growth [26].

The thermal characteristics of the as-dried nanopowders are shown in Fig. 2(a & b). The TG curve shows that the reactant precursor undergoes three stages of decomposition followed by the crystallization phases which resulted in 16% of total weight loss until 900 °C. More interestingly, an initial weight loss of only 10% that corresponds to the evaporation of surface water and the dehydration of the nanomaterial was noticed up to 400 °C, which appeared as two endothermic reactions at 100 and 360 °C in the DSC curve. A weight loss of 5% was perceived between 400 and 800 °C attributed to the decomposition of carbonates such as lanthanum carbonate which seems to be the reaction between $La(OH)_3$ with atmospheric CO_2 during the filtration process [27,28]. A final weight loss of about 1% above 700 °C is associated with the complete decomposition of the reactants, crystal lattice modifications and crystal growth, which can be seen as an exothermic reaction and fluctuations in DSC curve. The observed changes are in good agreement with the XRD results.

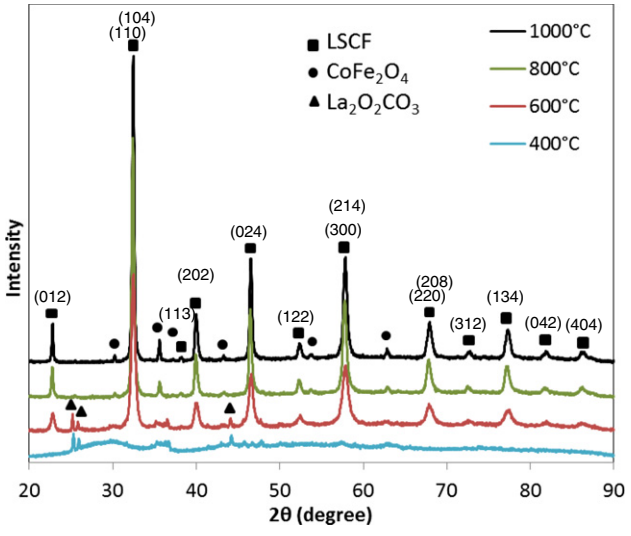

Fig. 1. XRD patterns of the LSCF nanostructures calcined at 400, 600, 800, and 1000 °C for 2 h.

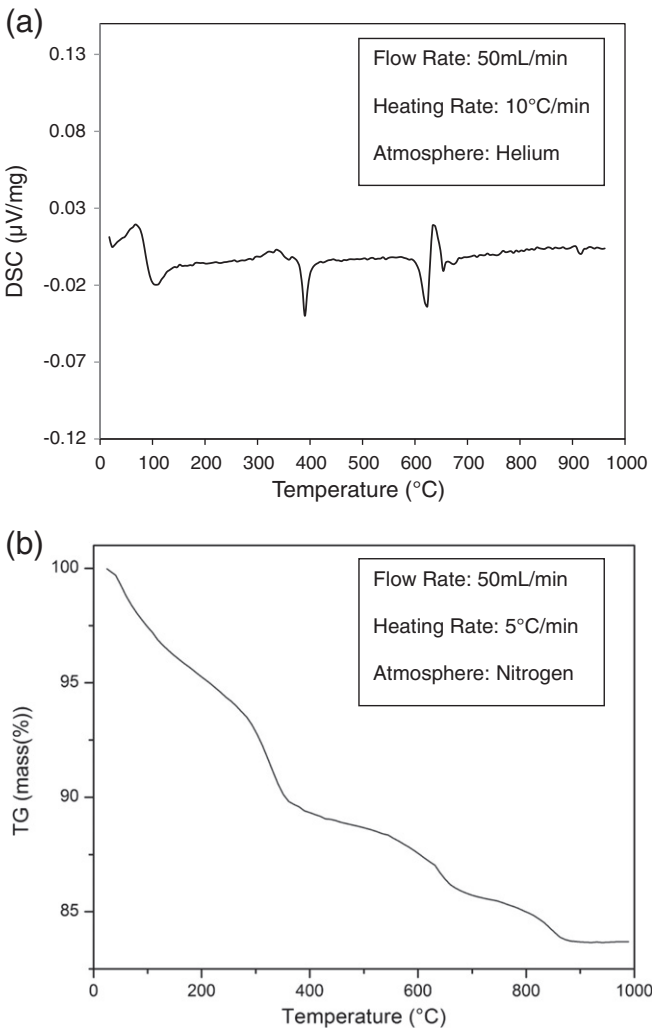

Fig. 2. (a) DSC and (b) TG curves of as-dried nanomaterials.

The TEM micrographs of the nanopowders calcined at 400,600, 800 and 1000 °C are presented in Fig. 3(a–f). The micrographs demonstrate the particle coarsening which occurred with the increase in the calcination temperature. The selected area diffraction (SAED) pattern of the nanostructures calcined at 400 °C shows an amorphous pattern and with the increase in calcination temperatures, becomes the ring diffraction patterns of polycrystalline materials. The SAED patterns (Fig. 3d and f), of the nanomaterials calcined at 1000 °C confirm the existence of LSCF and $CoFe_2O_4$ crystallites along with the XRD results. Fig. 4 shows spot chemical analysis of two different particles in nanopowders

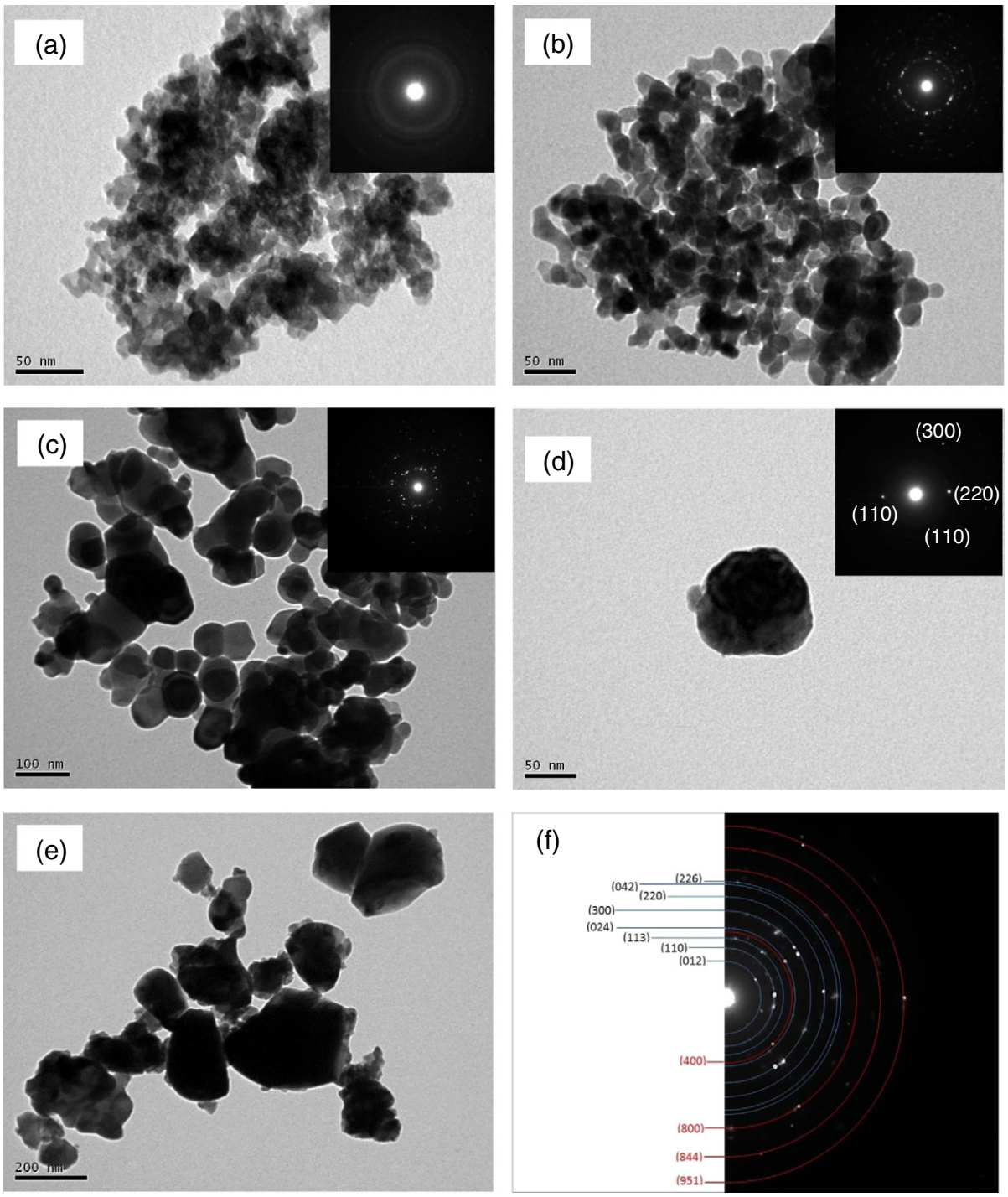

Fig. 3. TEM micrographs and SAED patterns of LSCF nanostructures calcined at (a) 400, (b) 600, (c) 800, and (d–f) 1000 °C for 2 h.

calcined at 800 °C by the EDS attached with TEM, which confirms the presence of LSCF and $CoFe_2O_4$ crystallites.

4. Conclusion

A low frequency ultrasound (42 kHz) assisted synthesis was employed to obtain the nanocrystalline LSCF perovskite. The X-ray diffraction analysis confirmed the presence of nanocrystalline LSCF and the formation of the secondary phase of $CoFe_2O_4$. The electron microscopic analysis of the nanostructures showed a uniform equi-axial shape and growth of LSCF particles until the calcination temperature of 800 °C. An average particle size less than 20 and 50 nm was obtained for LSCF calcined at 600 and 800 °C, respectively.

Acknowledgements

The authors acknowledge FONDECYT (3140180), and the Government of Chile, Santiago (Project Nos. 3140180 and 1130916) for the financial support in carrying out this project.

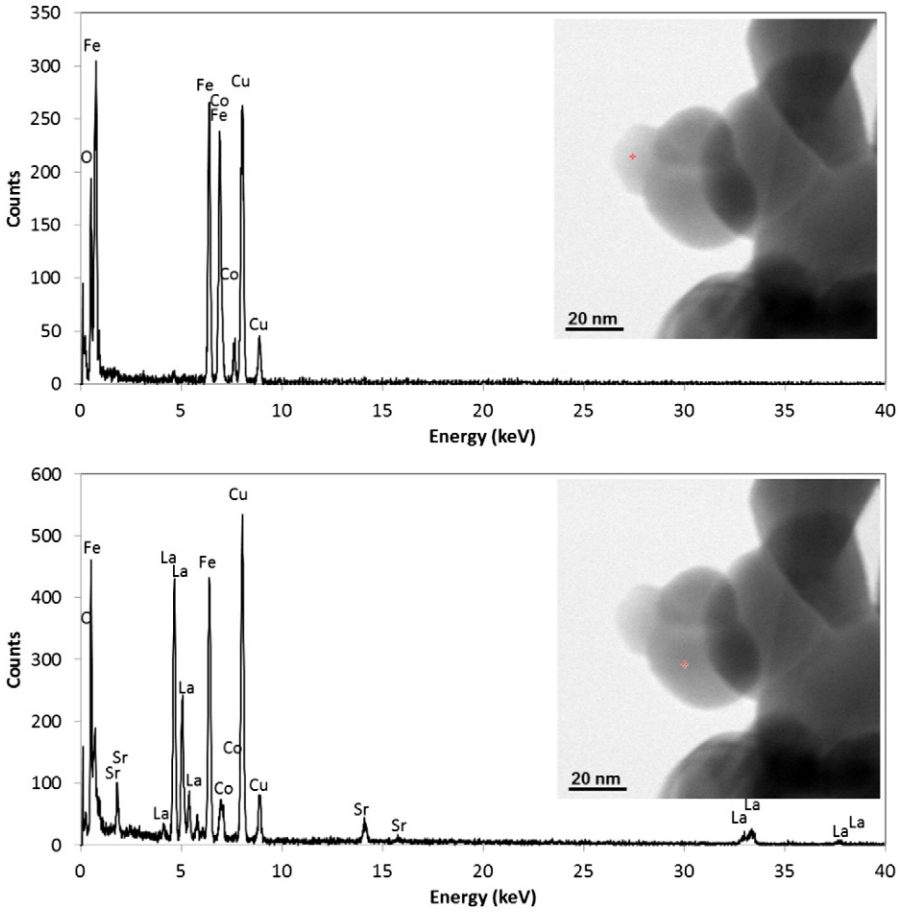

Fig. 4. TEM attached EDS spot analysis of LSCF nanopowders calcined at 800 °C for 2 h.

References

[1] J. Emmerlich, B.M. Linke, D. Music, J.M. Schneider, Solid State Ionics 255 (255) (2014) 108–112.
[2] S.J. Kim, G.M. Choi, Solid State Ionics 262 (2014) 303–306.
[3] X. Wang, F. He, Z. Chen, A. Atkinson, J. Eur. Ceram. Soc. 34 (2014) 2351–2361.
[4] E. Magnone, J.H. Park, A. Gen, Mater. Lett. 127 (2014) 56–58.
[5] Y. Teraok, H.M. Zhang, N. Yamazoe, Chem. Lett. 9 (1985) 1367–1370.
[6] L.W. Tai, M.M. Nasrallah, H.U. Anderson, D.M. Sparlin, S.R. Sehlin, Solid State Ionics 76 (1995) 259–271.
[7] A. Fossdal, M. Menon, I. Waernhus, K. Wiik, M.A. Einarsrud, T. Grande, J. Am. Ceram. Soc. 87 (2004) 1952–1958.
[8] R.V. Côrte, L. Conceição, M.M.V.M. Souza, Ceram. Int. 39 (2013) 7975–7982.
[9] M. Zawadzki, Trawczynski, Catal. Today 176 (2011) 449–452.
[10] L. Conceicao, A.M. Silva, N.F.P. Ribeiro, M.M.V.M. Souza, Mater. Res. Bull. 46 (2011) 308–314.
[11] L. Ge, W. Zhou, R. Ran, Z. Shao, S. Liu, J. Alloys Compd. 450 (2008) 338–347.
[12] A. Akbari-Fakhrabadi, R.E. Avila, H.E. Carrasco, S. Ananthakumar, R.V. Mangalaraja, S.H. Chan, Mater. Focus 2 (2013) 188–194.
[13] M. Zawadzki, H. Grabowska, J. Trawczyński, Solid State Ionics 181 (2010) 1131–1139.
[14] A. Dutta, J. Mukhopadhyay, R.N. Basu, J. Eur. Ceram. Soc. 29 (2009) 2003–2011.
[15] M. Ghouse, Y. Al-Yousef, A. Al-Musa, M.F. Al-Otaibi, Int. J. Hydrog. Energy 35 (2010) 9411–9419.
[16] Y. Zeng, Y.S.: Lin, S.L. Swartz, J. Membr. Sci. 150 (1998) 87–98.
[17] M.A. Haider, A.J. Capizzi, M. Murayama, S. McIntosh, Solid State Ionics 196 (2011) 65–72.
[18] A. Galenda, M.M. Natile, A. Glisenti, J. Mol. Catal. A 282 (2008) 52–61.
[19] L.M.P. Garcia, D.A.M. Macedo, G.L.S. Souza, F.V.M. Motta, C.A.P. Paskocimas, R.M.N. Nascimento, Ceram. Int. 39 (2013) 8385–8392.
[20] N. Das, D. Bhattacharya, A. Sen, H.S. Maiti, Ceram. Int. 35 (2009) 21–24.
[21] G. Pang, X. Xu, V. Markovich, S. Avivi, O. Palchik, Y. Koltypin, G. Gorodetsky, Y. Yeshurun, H.P. Buchkremer, A. Gedanken, Mater. Res. Bull. 38 (2003) 11–16.
[22] C.R. Michel, E.R. Lopez, H.R. Zea, Mater. Res. Bull. 41 (2006) 209–216.
[23] B.G. Pollet, Int. J. Hyd. Energy 35 (2010) 11986–12004.
[24] P. Sathishkumar, R.V. Mangalaraja, H.D. Mansilla, M.A. Gracia-Pinilla, S. Anandan, Appl. Catal. B Environ. 160–161 (2014) 692–700.
[25] B.D. Cullity, Elements of X-ray diffraction, 2ed, Addison-Wesley, MA, 1978.
[26] C. Ding, K. Sato, J. Mizusaki, T. Hashida, Ceram. Int. 38 (2012) 85–92.
[27] R.I. Fertout, M. Ghelamallah, S. Kacimi, Adv. Mat. Phys. Chem. 2 (2012) 31–36.
[28] B. Bakiz, F. Guinneton, M. Arab, A. Benlhachemi, J.R. Gavarria, M. J. Cond. Mat. 12 (2010) 60–67.